Proc. IEEE Conference on Computer Vision and Pattern Recognition, San Francisco, 27-34.

Scale Space Localization, Blur, and Contour-Based Image Coding

James H. Elder

Computer Science Division
NEC Research Institute
Princeton, NJ 08540

Steven W. Zucker

Centre for Intelligent Machines
McGill University
Montréal, Québec, Canada H3A 2A7

Abstract

We have recently proposed a scale-adaptive algorithm for reliable edge detection and blur estimation [4]. The algorithm produces a contour code which consists of estimates of position, brightness, contrast and blur for each edge point in the image. Here we address two questions: **1.** *Can scale adaptation be used to achieve precise localization of blurred edges?* **2.** *How much of the perceptual content of an image is carried by the 1-D contour code? We report an efficient algorithm for subpixel localization, and show that local scale control allows excellent precision even for highly blurred edges. We further show how local scale control can quantitatively account for human visual acuity of blurred edge stimuli. To address the question of perceptual content, we report an algorithm for inverting the contour code to reconstruct an estimate of the original image. While reconstruction based on edge brightness and contrast alone introduces significant artifact, restitution of the local blur signal is shown to produce perceptually accurate reconstructions.*

1 Introduction

Many algorithms for stereo correspondence, pose estimation and object recognition use image contours as matching primitives. Here we address two problems with this approach. First, in real scenes, broad variation in contrast and local blurring cause errors and uncertainty in edge detection, making these contours unreliable and degrading performance in higher-level computations. Second, there is clearly a great deal of information in an image which is not captured by its edge map: it is unclear why we should insist on ignoring this information when performing higher-level tasks.

One possible conclusion is that contours are simply a bad way of coding images for subsequent processing. In this paper we take a more optimistic view: that a contour code can potentially be quite reliable and perceptually nearly complete, if care is taken in how we detect and represent the local edges that constitute the code.

2 Local Scale Control

While edge detectors are typically designed to recover step discontinuities in an image (e.g. [1, 9]), the boundaries of physical structures in the world generally do not project to the image as step discontinuities, but as blurred transitions corrupted by noise. Variations in reflectance and lighting generates a broad range of contrasts, while defocus, shadows and shading generate a broad range of local blur.

Consider Fig. 1 (top). On the left is shown the edge map generated by the Canny edge detector [1], where the scale parameter has been tuned to detect the details of the mannequin. At this relatively small scale, the contour of the shadow cannot be reliably resolved. On the right is shown the edge map generated when scale is tuned to detect the contour of the shadow. At this larger scale, the details of the mannequin are blurred out, and the contour of the shadow is fragmented at the section of high curvature under one arm.

This example demonstrates that detecting and modeling the edges in a natural image requires a multi-scale approach. Multi-scale theories generally require the integration of filter responses over many scales [1, 12] or feature-tracking through a continuous 3-D scale space, in which image contours are coded as two-dimensional surfaces [8, 10, 22]. Here we describe a theory for local scale control that determines a unique scale for local estimation at each point in an image [3, 4], thus avoiding the problem of combining filter responses or tracking features through scale space.

Edge detection typically involves the estimation of 1st and perhaps 2nd derivatives of the luminance function, followed by selection of zero crossings or extrema. If these derivative estimates are unreliable, the selected edges will be incorrect. Local scale control is based on the observation that sensor noise properties and operator norms can be used to determine a unique minimum scale at which derivative estimates can be used to make reliable local logical inferences. We call this unique scale the *minimum reliable scale* for the estimation.

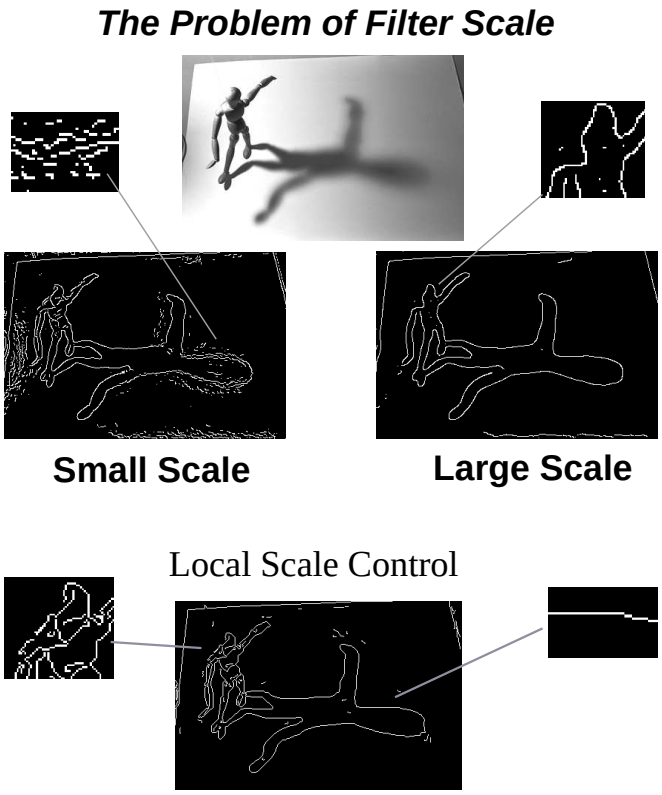

Figure 1: **Top:** Output of Canny edge detector for different filter scales. **Bottom:** Edges recovered by local scale control.

Ensuring reliability in terms of sensor noise does not account for the danger of incorrect assertions due to the influence of scene events nearby in the image, which in any band-limited system must be an increasing function of scale. By selecting the minimum of the set of reliable scales, we ensure reliability relative to sensor noise, while minimizing distortion from nearby image events and deviations from our local edge model.

The key to the local scale control algorithm is the prior computation of a significance function $s(\sigma)$ which determines the lower bound on filter response as a function of filter scale σ, below which the response cannot be used reliably. The significance function depends on the L_2 norm of the filter, the statistics of the sensor noise, and the property of the response that we wish to exploit.

Using steerable Gaussian derivative filters [6, 17], our method for edge detection depends upon the reliable detection of a non-zero gradient $r_1^{\theta_M}(x, y, \sigma_1)$ in the luminance function, and the reliable inference of the *sign* of the 2nd derivative $r_2^{\theta_M}(x, y, \sigma_2)$ of the luminance function in the gradient direction θ_M. Each of these inferences determines a specific significance function. By reliable here we mean that the likelihood of making at least one decision error over an entire image is less than a standard tolerance of 5%. For Gaussian i.i.d. sensor noise and an image of standard size ($\approx 256 \times 384$), the sign of response of a unit-power linear filter is reliable by this criterion if its response magnitude exceeds $5\sigma_n$, where σ_n is the standard deviation of the sensor noise. A Gaussian derivative filter is generally not unit power, and since the L_2 norm of the filter varies with filter scale, the significance function for the filter varies accordingly.

The significance functions for asserting a non-zero gradient, and for determining the sign of the 2nd derivative in the gradient direction are [3, 4] [1]

$$s_1(\sigma_1) = 3\sigma_n/\sqrt{\pi}\sigma_1^2 \qquad s_2(\sigma_2) = 5\sigma_n/2\sqrt{2\pi}\sigma_2^3$$

where σ_1 and σ_2 are the scales of the Gaussian 1st and 2nd derivative filters, respectively.

To apply local scale control to the detection of blurred edges, we model an edge as a step function $Au(x) + B$ of unknown amplitude A and pedestal offset B, aligned, for convenience, with the y-axis of our coordinate frame. The focal or penumbral blur of this edge is modelled by a Gaussian blur kernel, $g(x, y, \sigma_b) = \frac{1}{2\pi{\sigma_b}^2} e^{-(x^2+y^2)/2{\sigma_b}^2}$ of unknown scale constant σ_b. Sensor noise $n(x, y)$ is modeled as a stationary, additive, zero-mean white noise process with standard deviation σ_n. The complete edge model is thus:

$$(A/2)(erf(x/\sqrt{2}\sigma_b) + 1) + B + n(x, y). \qquad (1)$$

The prior construction of significance functions allows the minimum reliable scale for each estimation to be determined at each point as the image is processed. The situation for gradient estimation at an edge is shown in Fig. 2 (top left). Although both the gradient response $r_1^{\theta_M}$ and the significance function $s(\sigma_1)$ decline with increasing scale, the significance function declines much more quickly. The scale at which the two curves intersect is the minimum reliable scale for gradient estimation. In our experiments we attempt only to stay close to the minimum reliable scale by computing estimates at octave intervals of scale, at each point using the smallest scale at which the estimate exceeds the significance function, i.e., for gradient estimation, $\hat{\sigma}_1(x, y) = \inf\{\sigma_1 : r_1^{\theta_M}(x, y, \sigma_1) > s_1(\sigma_1)\}$.

The importance of the 2nd derivative in localizing blurred edges is illustrated in Fig. 2. Fig. 2 (top right) shows the luminance profile through the edge of the mannequin's shadow. Fig. 2 (middle right) shows the gradient magnitude along the cross-section, and Fig. 2 (middle left) shows the minimum reliable scales at which the gradient was estimated. Note how

[1] While gradient estimation is a nonlinear operation, stochastic inequalities can be used to compute a slightly conservative estimate of the significance function.

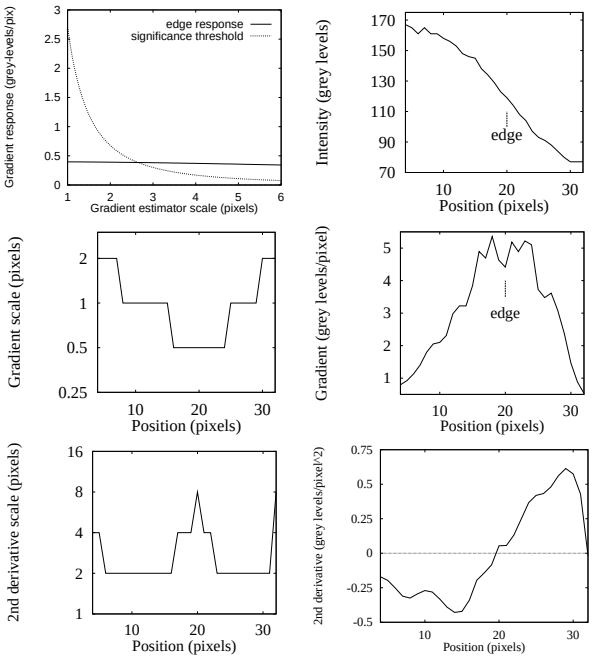

Figure 2: **Top left:** The intersection of the significance function $s_1(\sigma_1)$ with the gradient response $r_1^{\theta_M}(\sigma_1)$ determines the minimum reliable scale for gradient estimation. **Top right:** Cross section of image across shadow boundary. **Middle left:** Minimum reliable scale for the gradient estimate. **Middle right:** Estimated gradient magnitude. **Bottom left:** Minimum reliable scale for the 2nd derivative estimate **Bottom right:** Estimated directional 2nd derivative. A unique zero-crossing localizes the edge.

the scale of estimation automatically adapts as the strength of the signal varies. Although this allows the gradient to be reliably detected as non-zero over this cross-section, the response is not unimodal: there are in fact 5 maxima in the gradient along the cross section of the edge. Marking edges at extrema in the gradient function would clearly lead to multiple separate responses to this single edge.

Fig. 2 (bottom right) shows the estimated 2nd derivative steered in the gradient direction, and Fig. 2 (bottom left) shows the minimum reliable scales for these estimates. Note again how scale automatically adapts as the signal varies in strength: larger scales are needed near the centre of the edge where the luminance function is nearly linear. Despite the rockiness of the gradient response, the adaptive 2nd derivative response provides a unique zero-crossing to localize the edge. The key here is that local estimation at the minimum reliable scale guarantees that the sign of the 2nd derivative estimate is reliable, and hence that the zero-crossing is unique. The number of peaks in the gradient response, on the other hand, depends on the

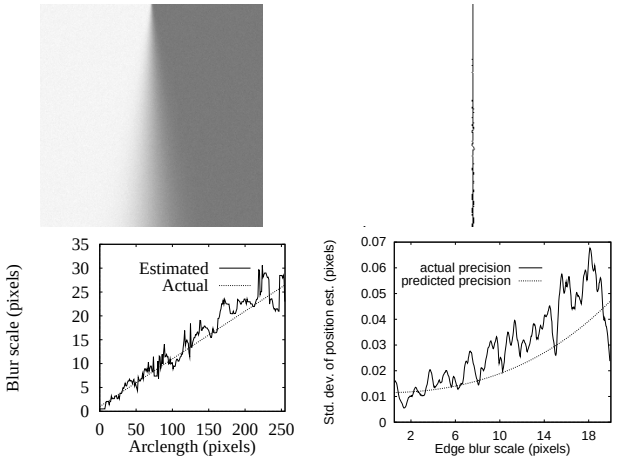

Figure 3: **Top left:** The blur grade is linear, ranging from $\sigma_b = 1$ pixel to $\sigma_b = 26.6$ pixels. Parameters (see Eqn. 1): $A = B = 85$ grey levels, $\sigma_b \in [1, 26.6]$ pixels, $\sigma_n = 1.6$ grey levels. **Top right:** Edges detected by local scale control. **Bottom left:** Estimated blur scale σ_b. **Bottom right:** Predicted and measured localization precision Δx.

blur of the edge, and is not revealed in the response of the operator at any single point: ensuring the uniqueness of a gradient maximum is not a local problem. Thus the reliable detection and localization of blurred edges requires both gradient and 2nd derivative estimation.

We tested the local scale control algorithm for edge detection on the synthetic image of Fig. 3, a vertical edge blurred by a space-varying Gaussian kernel, corrupted by Gaussian i.i.d. noise. Five scales were used for gradient estimation ($\sigma_1 \in \{0.5, 1, 2, 4, 8\}$ pixels), six for 2nd derivative estimation ($\sigma_2 \in \{0.5, 1, 2, 4, 8, 16\}$ pixels). Fig. 3 (top right) shows the edges detected by the local scale control algorithm. The edges are reliably and uniquely detected over a wide range of blur. Fig. 1 (bottom) shows the edges detected in the image of the mannequin and shadow. Both the fine detail of the mannequin and the complete contour of the shadow are resolved, without spurious responses to the smooth shading gradients on the ground surface. We emphasize that this is achieved by a single system with no input parameters other than the second moment of the sensor noise.

3 Blur Estimation

Local scale control may also be applied to the estimation of focal blur. While excellent passive techniques for blur estimation have been developed, these typically require densely-textured surfaces varying slowly in depth (e.g. [5, 13, 16]) and are therefore not suited for complex images (e.g. Fig. 4), where each local neighbourhood may contain many depth

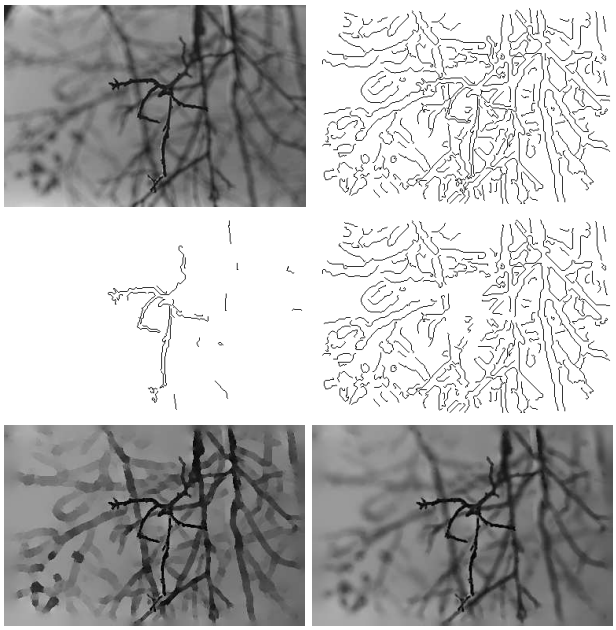

Figure 4: **Top left:** A photograph of tree branches with small depth of field ($f/3.5$) and near focus. **Top right:** Edge map computed by local scale control. **Middle left:** Foreground structure (focused contours). **Middle right:** Background structure (defocused contours). **Bottom left:** Reconstructed luminance terrain. **Bottom right:** Reconstructed, reblurred result.

discontinuities. In such cases, blur estimates can only be made where structure exists, and must be computed as locally as possible. Contour-based blur estimation at the minimum reliable scale is naturally suited to the task.

In our local scale control method, blur scale σ_b is estimated by computing the distance between extrema of opposite sign in the 2nd derivative response along the gradient direction, and then correcting for the blur induced by the estimation itself [3, 4]. Fig. 3 (bottom left) shows a plot of the estimated and actual blurs of the synthetic test image. While the resulting pointwise blur estimates are noisy, they provide an approximately unbiased estimate of the blur scale of the edge. This method for blur estimation was applied to the problem of segmenting the tangle of branches shown in Fig. 4. Fig. 4 (middle left) and (middle right) show the extracted foreground (focused) and background (defocused) structure, respectively.

4 Spatial Precision

While in the preceding experiments, the local scale of estimation was adapted to allow reliable localization to 1 pixel resolution, many applications (e.g. stereo matching) benefit from greater precision. Here we consider how local scale control can be used to achieve more precise localization.

The *expected* response of a 2nd derivative operator to the blurred edge modeled by Eqn. 1 is given by

$$\hat{r}_2^x(x,y,\sigma_2) = -\frac{Ax}{\sqrt{2\pi}(\sigma_b^2+\sigma_2^2)^{3/2}} e^{-x^2/2(\sigma_b^2+\sigma_2^2)}.$$

For $|x| << \sqrt{\sigma_b^2+\sigma_2^2}$, this response can be modeled by the 1st-order Taylor series approximation:

$$\hat{r}_2^x(x,y,\sigma_2) \approx -\frac{Ax}{\sqrt{2\pi}(\sigma_b^2+\sigma_2^2)^{3/2}}$$

The expected location of the zero-crossing in the 2nd derivative is at $x=0$. The *actual* 2nd derivative response will be perturbed by the response $\tilde{r}_2^x(x,y,\sigma_2)$ to the noise component of the model. Since the 2nd derivative filter is bandpass, the noise response can, for $|x| << \sigma_2$, be modeled by a 0th order Taylor series approximation: $\tilde{r}_2^x(x,y,\sigma_2) \approx r_2^x(0,y,\sigma_2)$. The actual zero-crossing in the noisy signal occurs when $\hat{r}_2^x(x,y,\sigma_2) + \tilde{r}_2^x(x,y,\sigma_2) = 0$, i.e. at

$$x_z \approx \frac{\sqrt{2\pi} r_n}{A}(\sigma_b^2+\sigma_2^2)^{3/2}$$

where $r_n = r_2^x(0,y,\sigma_2)$. r_n is a Gaussian random variable with standard deviation $\sigma_n ||g_2(x,y,\sigma_2)||_2$, where $||g_2(x,y,\sigma_2)||_2 = \sqrt{3/\pi}/4\sigma_2^3$ [3]. Thus the standard deviation of the zero crossing location is given by

$$\Delta x \approx \frac{\sqrt{6}\sigma_n}{4A}(1+(\sigma_b/\sigma_2)^2)^{3/2}. \qquad (2)$$

For this hypothetical case of an isolated blurred edge of infinite length, precision improves monotonically with filter scale, and in the limit is independent of blur, depending only on the signal-to-noise ratio A/σ_n. For real images, due to the finite extent of the edge and the presence of nearby edges, the optimal scale will be finite. In real systems, efficiency constraints will also impose an upper bound on maximum filter scale. In practice, therefore, precision generally *will* degrade with increased blur.

A typical situation is depicted in Fig. 5 (left). Here the actual location of the edge is at $x=0$, between pixels x_+, where $r_2^{\theta_M} > 0$ and x_-, where $r_2^{\theta_M} < 0$. Local scale control can be used to estimate $r_2^{\theta_M}$ at intermediate locations to generate a more precise estimate x_z of the position of the edge. Equation 2 imposes an upper bound on the precision attainable.

To compute x_z, local scale control is used to estimate $r_2^{\theta_M}$ at $x_? = (x_+ + x_-)/2$. Since the expected response of $r_2^{\theta_M}(x,y,\sigma_2)$ approaches 0 near the edge, there may be no scale at which a reliable estimate can be made. In this case, we select the scale which maximizes the signal-to-noise ratio $|r_2^{\theta_M}(x,y,\sigma_2)|/s_2(\sigma_2)$. If the estimate is positive, we set $x_+ = x_?$, otherwise, we set $x_- = x_?$. This process is iterated to determine

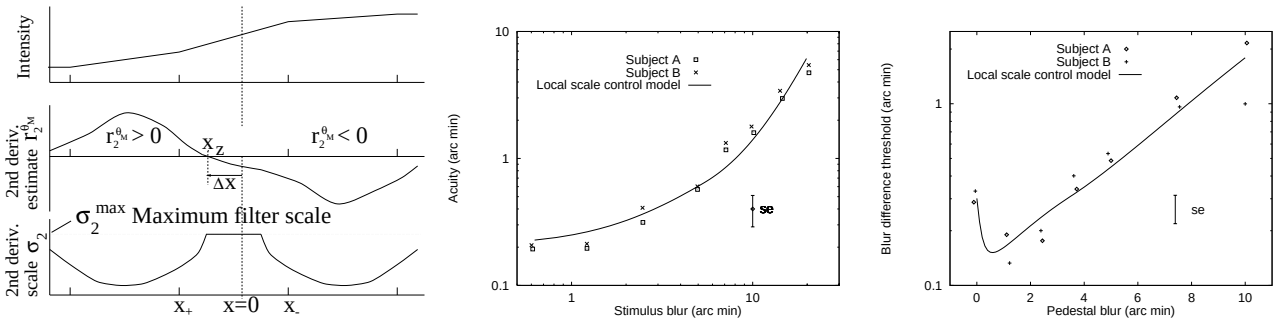

Figure 5: **Left:** Subpixel localization using local scale control. **Middle:** Modelling human visual acuity Δx as a function of blur scale σ_b. Data from [20]. Fitted local scale control model shown as solid line. **Right:** Modelling blur discriminability $\Delta\sigma_b$ for human vision as a function of pedestal blur scale σ_b. Data from [20]. Fitted local scale control model shown as solid line.

x_z to a preset precision (0.001 pixels).

This algorithm was tested on the graded blur image of Fig. 3. Fifteen samples of the image were used, each corrupted by independent samples of additive Gaussian noise. In this way, estimates of the standard deviation Δx of the estimated edge position were obtained as a function of the blur scale σ_b of the edge. The results are shown in Fig. 3 (bottom right). The actual performance of the algorithm is very close to that predicted by Eqn. 2. Precision of less than 1/20 of a pixel is attainable even for highly blurred edges.

While localization accuracy is very high for this synthetic image, systematic errors will be introduced by contour curvature, smooth undulations of the luminance function near the edge, and nearby edges in the image. Maintaining precise *and* accurate measurements in this more realistic context remains an open problem. However, since these biases are deterministic, the local scale control algorithm can potentially be used to compute with high accuracy the location of an object *relative* to a previous location. This is useful for motion and stereo computation and for robotics applications which require repositioning of objects to a set of canonical positions.

5 Spatial Acuity in Human Vision

Watt & Morgan [20] have measured the precision with which human observers can align blurred edges and judge degree of blur, and have proposed a conceptual model they called MIRAGE to account for their data. In MIRAGE, performance is determined by a population response of filters over scale space.

The local scale control model has certain advantages over MIRAGE. First, while MIRAGE assumes that performance is limited by a late (post-filtering) source of visual noise, there is strong evidence that many psychophysical tasks are limited by noise early in the visual pathway (e.g. in the retina) [15,19]. Since reliability in local scale control is defined in terms of early (sensor) noise, the local scale control model is consistent with these psychophysical findings. Second, MIRAGE involves a complex, somewhat *ad hoc* set of rules for combining filter responses over scale space. In local scale control, estimates and decisions are made locally, at a unique, optimal scale. If consistent with the data, local scale control would provide a relatively parsimonious account of spatial acuity, with a clear algorithmic implementation.

As in MIRAGE, we assume visual noise to be additive, i.i.d. and Gaussian. For the localization task, the local scale control theory generates the following acuity model:

$$\Delta x = \frac{2C((\sigma_b/\sigma_2)^2 + (\sigma_o/\sigma_2)^2 + 1)^{3/2}}{erf(6/\sqrt{2}\sigma_2)}$$

This is a direct adaptation of Eqn. 2, with minor modifications to account for the blur induced by the optics of the eye (σ_o), and truncation of the stimulus by a rectangular window (which generates the erf() factor). The constant C is proportional to the inverse of the signal-to-noise ratio of the stimulus, and embodies several constant factors required to convert to the measure of visual acuity employed by Watt and Morgan.

The model indicates that acuity will be determined in part by maximum filter scale. Since there is considerable disagreement in the physiological and psychophysical literature on what this upper bound should be, we leave it as a free parameter in fitting the model to the data. The other free parameter is the scaling factor C, proportional to the unknown level of intrinsic visual noise. The optical blur is fixed at a standard value of $\sigma_o = 0.3$ arc min. The fit of the model to the data of Watt & Morgan for spatial acuity as a function of edge blur is shown in Fig. 5(middle). The fit of the model is well within the standard error of the data.

Using a similar local scale control analysis, it is straightforward to derive a predictive model for the

Filter	Bandwidth (octaves)	Max. Scale (min arc)	Noise Constant (C)
$g_2(x, y, \sigma_2)$	1.8	8.7	0.23
$g_3(x, y, \sigma_3)$	1.4	7.1	0.25

Table 1: Model parameters predicted by MSE fits to acuity and blur discrimination data.

estimation of blur scale:

$$\Delta\sigma_b = \frac{\sqrt{5}eC((\sigma_b/\sigma_3)^2 + (\sigma_o/\sigma_3)^2 + 1)}{2erf(6/\sqrt{2}\sigma_3)}$$

In this model, blur discrimination is determined by the third Gaussian derivative operator, and the upper bound on filter scale is again left as a free parameter. The fit of the model to the data of Watt and Morgan is shown in Fig. 5(right). The model closely follows the data, including the deterioration in acuity at low levels of stimulus blur caused by the optical blur limit.

Since these two models were fit to these two distinct sets of data independently, they provide independent predictions for the free parameters of the models. These are summarized in Table 1. First note that the modeling predicts a higher upper bound on the scale of the 2nd derivative operator than for the third derivative operator. This is consistent with physiological observations that spatially narrow-band neurons in striate cortex tend to have higher peak frequencies [18]. Second, note that these two independent experiments predict nearly identical values for C, the intrinsic visual noise constant.

6 Inverting the Contour Code

The idea that the primary purpose of early visual coding is to detect and represent contour dates to the experiments of Mach and the proposition of lateral inhibition. This idea does not explain our perception of brightness, colour and shading between contours. 60 years ago, Werner provided some possible clues, in what is generally regarded as the first "metacontrast" experiment [21]. Werner showed that by interrupting the formation of a complete bounding contour, one could prevent observers from perceiving the colour of the object which this contour bounds. Many subsequent metacontrast experiments have elaborated this finding (e.g. [14]), leading to the hypothesis of a contour-based "filling-in" process responsible for our perception of surface brightness and colour.

Computer vision work on this issue has addressed the question of whether a 2-D signal can be recovered perfectly from a scale space representation of its zero-crossings (e.g. [7, 11]). While this question is of theoretical interest, since a scale space representation of the zero-crossings of an image is itself 2-D, such a code does not necessarily imply any simplification of representation. A more dramatic question is whether an image can be represented to high fidelity with a

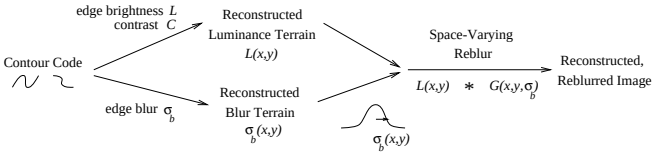

Figure 6: Inverting the contour code. Perceptually accurate reconstruction requires contour brightness, contrast and blur coding. Luminance and blur terrains are reconstructed and then combined by space-varying convolution.

contour code which is 1-D, i.e. where a unique scale is employed at each contour point, as in local scale control. This is the question we address here.

The contour code produced by local scale control represents estimated position, brightness, contrast and blur scale at each edge point in an image. We present a diffusion algorithm for inverting this 1-D code to reconstruct a 2-D image. The idea of using a diffusion process to reconstruct an image from its edges was first advanced by Carlsson for the purpose of image compression [2]. He proposed to code the intensity on either side of each edge, and interpolate image intensity between contours by diffusing intensity estimates from these edges. Using a multi-grid method, the reconstruction can be computed quite efficiently.

Carlsson actually used a sub-sampled version of the original image to further constrain the reconstruction, so it is unclear from his results how much perceptual information was actually contained in the contours. Also, although Carlsson achieved his objective of computing intelligible reconstructions, the results were far from perfect. There are many possible reasons for the perceptual distortions, including lack of rotation invariance in estimation (only vertical and horizontal edges were considered) and failure to adapt the scale of estimation to the local image structure.

We have implemented a multi-grid diffusion method for reconstructing images solely from a contour code computed by local scale control. The algorithm solves for the steady-state solution of the heat equation, with image intensity as the diffusive quantity and brightness and contrast estimates at contour points as boundary conditions. The results of this algorithm are shown in the bottom left frames of Figs. 4, 7, 8 and 9. Intermediate stages of a single-grid reconstruction are shown in the middle frames of Fig. 7. While the results are quite good, even this rotation invariant, scale-adaptive method fails to reconstruct the original images without artifact: the results appear more like paintings than photographs.

The key problem here seems to be the deblurring inherent in the reconstruction algorithm: note how shadows, shading and defocused contours appear quite

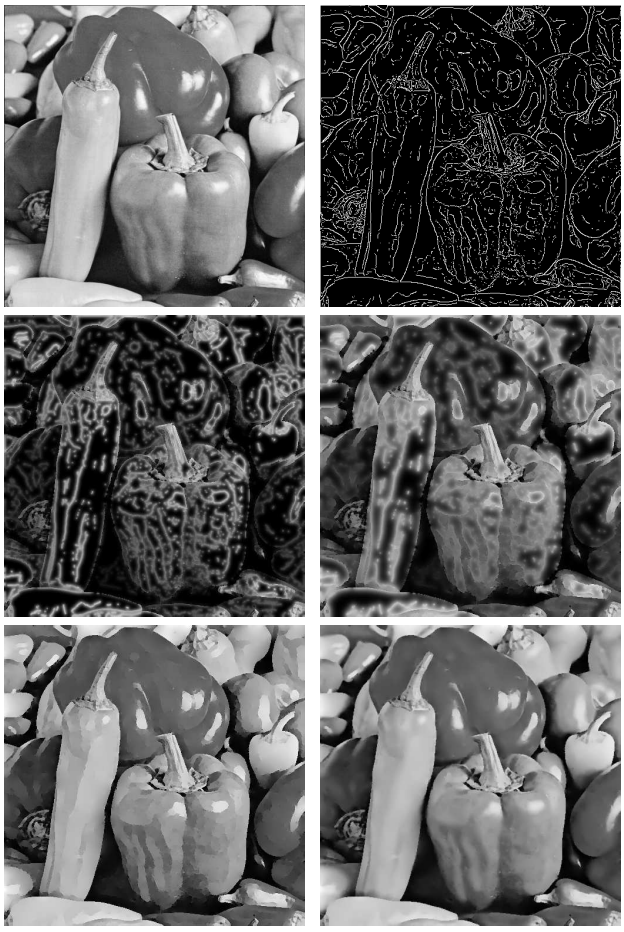

Figure 7: **Top left:** Original image. **Top right:** Contours. **Middle:** Intermediate stages of single-grid reconstruction. **Bottom left:** Reconstructed luminance function. **Bottom right:** Reblurred result.

unnatural. It appears that obtaining perceptually accurate reconstructions from the contour code may depend upon accurate *re*blurring of the reconstructed luminance function.

Restoring the local blur information to the reconstructed image is problematic since we only have blur estimates at contour points, yet we need to smoothly reblur the image not just at these points, but in the general neighbourhood of each point, and the size of this neighbourhood depends upon the local degree of blur.

There is an elegant solution to this problem (Fig. 6). We again solve the heat equation over the image, but where the diffusive quantity is blur scale, rather than luminance, and the boundary conditions are the local estimates of blur scale along the detected contours. In this way, a blur surface is constructed which assigns a blur scale to each pixel in the image. The reconstructed luminance function can then be re-

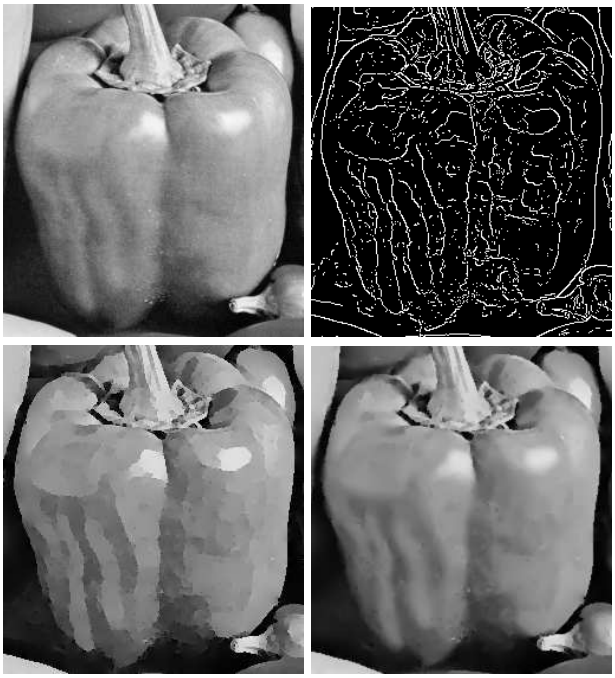

Figure 8: **Top left:** Original. **Top right:** Contours. **Bottom left:** Luminance reconstruction. **Bottom right:** Reblurred reconstruction.

Figure 9: **Top left:** Original image. **Top right:** Contours. **Bottom left:** Reconstructed luminance function. **Bottom right:** Reblurred result.

blurred with an isotropic Gaussian blur kernel with space-varying blur scale, where the blur scale at each pixel is selected from the corresponding point on the reconstructed blur surface. The results of the complete reconstruction/reblurring algorithm are shown in the bottom right frames of Figs. 4, 7, 8 and 9. The results are perceptually very close to the original images.

7 Conclusion

To support higher-level computations, an early visual representation must be reliable, precise and informative. We have argued that a contour code computed by local scale control satisfies these requirements. This contour code represents position, brightness, contrast and blur at each edge point in an image. Edges are detected reliably over a broad range of contrast and blur scale, and local blur may be estimated accurately even for complex, highly discontinuous images. The local scale control model allows blurred edges to be localized to high precision, and appears to provide a simple explanation for human visual acuity of blurred stimuli. A simple and efficient method for inverting the contour code to reconstruct an estimate of the original image was presented. Restitution of local blur information was seen to be critical. The perceptual accuracy of the final reconstruction is evidence that the contour code captures the information needed for higher-level visual inference.

References

[1] J.F. Canny. Finding edges and lines in images. Master's thesis, MIT Artificial Intelligence Laboratory, 1983.

[2] S. Carlsson. Sketch based coding of grey level images. *Signal Processing*, 15:57–83, 1988.

[3] J. Elder. *The visual computation of bounding contours.* PhD thesis, McGill University, Dept. of Electrical Engineering, 1995.

[4] J. Elder and S.W. Zucker. Local scale control for edge detection and blur estimation. In *Lecture Notes in Computer Science*, New York, 1996. Proc. 4^{th} European Conf. on Computer Vision, Springer Verlag.

[5] J. Ens and P. Lawrence. Investigation of methods for determining depth from focus. *IEEE Trans. Pattern Anal. Machine Intell.*, 15(2):97–108, 1993.

[6] W.T. Freeman and E.H. Adelson. The design and use of steerable filters. *IEEE Trans. Pattern Anal. Machine Intell.*, 13(9):891–906, 1991.

[7] R. Hummel and R. Moniot. Reconstructions from zero crossings in scale space. *IEEE Trans. on Acoustics, Speech, and Signal Processing*, 37(12):2111–2130, 1989.

[8] J. Koenderink. The structure of images. *Biol. Cybern.*, 50:363–370, 1984.

[9] Y.G. Leclerc and S.W. Zucker. The local structure of image discontinuities in one dimension. *IEEE Trans. Pattern Anal. Machine Intell.*, 9(3):341–355, 1987.

[10] T. Lindeberg. Scale-space for discrete signals. *IEEE Trans. Pattern Anal. Machine Intell.*, 12(3):234–254, 1990.

[11] S. Mallat and S. Zhong. Characterization of signals from multiscale edges. *IEEE Trans. Pattern Anal. Machine Intell.*, 14:710–732, 1992.

[12] D. Marr and E. Hildreth. Theory of edge detection. *Proc. R. Soc. Lond. B*, 207:187–217, 1980.

[13] S.K. Nayar and N. Yasuo. Shape from focus. *IEEE Trans. Pattern Anal. Machine Intell.*, 16(8):824–831, 1994.

[14] M.A. Paradiso and K. Nakayama. Brightness perception and filling-in. *Vision Res.*, 7/8:1221–1236, 1991.

[15] D. G. Pelli. The quantum efficiency of vision. In C.B. Blakemore, editor, *Vision: Coding and Efficiency.* Cambridge University Press, Cambridge, UK, 1990.

[16] A.P. Pentland. A new sense for depth of field. *IEEE Trans. Pattern Anal. Machine Intell.*, 9(4):523–531, 1987.

[17] P. Perona. Deformable kernels for early vision. *IEEE Trans. Pattern Anal. Machine Intell.*, 17(5):488–499, 1995.

[18] L.G. Thorell R.L. DeValois, D.G. Albrecht. Spatial frequency selectivity of cells in the macaque visual cortex. *Vision Research*, 22:545–559, 1982.

[19] A.B. Watson. Neural contrast sensitivity. In M.S. Landy and J.A. Movshon, editors, *Computational Models of Visual Processing.* MIT Press, Cambridge, Mass., 1991.

[20] R.J. Watt and M.J. Morgan. The recognition and representation of edge blur: evidence for spatial primitives in human vision. *Vision Research*, 23(2):1465–1477, 1983.

[21] H. Werner. Studies on contour: I. qualitative analyses. *Amer. J. Psychol.*, 47:40–64, 1935.

[22] A. Witkin. Scale space filtering. *Proc. Int. Joint Conf. on Artif. Intell.*, pages 1019–1021, 1983.